Dalton Transactions

ROYAL SOCIETY OF CHEMISTRY

PERSPECTIVE

View Article Online
View Journal | View Issue

Cite this: *Dalton Trans.*, 2024, **53**, 18803

Mechanistic insights on C(acyl)–N functionalisation mediated by late transition metals

Vivek G. Pillai, Kaycie R. Malyk and C. Rose Kennedy *

Received 25th June 2024,
Accepted 2nd August 2024

DOI: 10.1039/d4dt01829j

rsc.li/dalton

The carboxamide functional group has a privileged role in organic and biological chemistry due to its prevalence and utility across synthetic and natural products. Due to $n_N \rightarrow \pi^*_{CO}$ delocalisation, amides and related functional groups are typically kinetically resistant to degradation. Nonetheless, over the past decade, transition metal catalysis has transformed our ability to utilise molecules featuring C(acyl)–N units as reactants. Alongside the burgeoning catalytic applications ranging from CO_x utilisation to small molecule synthesis, elucidation of the underlying mechanisms remains a critical ongoing effort. Herein, we aggregate and analyse current understanding of the mechanisms for C(acyl)–N functionalisation of amides and related functional groups with a focus on recent developments involving mechanisms unique to the late transition metals. Discussion is organized around three general mechanistic manifolds: redox-neutral mechanisms, $2e^-$ redox-cycling mechanisms, and mechanisms involving $1e^-$ redox steps. For each class, we focus on reactions that directly involve a transition metal mediator/catalyst in the C(acyl)–N cleavage step. We conclude with an outlook on the outstanding ambiguities and opportunities for innovation.

1. Introduction

The carboxamide functional group is of central importance across fields of chemistry and biology. The amidic C(acyl)–N motif is found in a wide range of organic molecules, pharmaceuticals, agrochemicals, and natural products in addition to forming the essential linkages in proteins and peptides. A simple search using SciFinder^n returns 6.9 million carboxamide-containing molecules with pharmacological activity and 7.6 million with agrochemical applications. Additionally, carboxamides are typically cheap, readily available, and straightforward to handle making them attractive functional groups for synthetic chemistry.

A dominant feature enabling the prevalence of the carboxamide motif arises from the 3-center 4-π delocalisation across the amidic unit (described as n(N)→π*(CO) delocalisation), which results in resonance stabilization values of 15–20 kcal mol^{-1} and partial C(acyl)–N double-bond character.[1,2] The

Department of Chemistry, University of Rochester, Rochester, NY 14627, USA.
E-mail: c.r.kennedy@rochester.edu

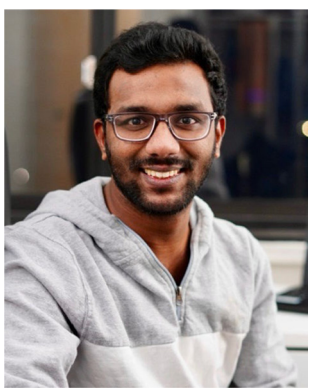

Vivek G. Pillai

Vivek G. Pillai earned a BS-MS degree in Chemistry from the Indian Institute of Science Education and Research (IISER), Thiruvananthapuram, India, in 2021. He is currently pursuing his Ph.D. at the University of Rochester under the guidance of Dr Rose Kennedy. His research focuses on elucidating the mechanisms underlying nickel-catalyzed amide C(acyl)–N bond activation.

Kaycie R. Malyk

Kaycie R. Malyk received her B.S. in Chemistry from the State University of New York at Fredonia in 2020. She is currently pursuing her Ph.D. under the supervision of Dr Kennedy at the University of Rochester. Her research is focused towards understanding the mechanisms and chemoselectivity-determining features of C(acyl)–N electrophiles in Ni-catalyzed reactions.

kinetic and thermodynamic penalty for cleaving this C–N bond thus limits the synthetic transformations accessible from simple amides compared to other carboxylic acids derivatives such as acyl halides or anhydrides. As a result, catalysis (especially transition metal catalysis) plays an important role in expanding the synthetic utility of amides and related *N*-acyl functional groups. Detailed understanding of the mechanisms by which transition metals enable C(acyl)–N functionalisation is thus essential to drive continued innovation in methodology development.

In this *Perspective*, we have attempted to aggregate and analyse current understanding of the mechanisms for C(acyl)–N functionalisation of amides and related functional groups. We note that molecules bearing stereoelectronically distorted C(acyl)–N units are often described in the literature as "non-planar amides" or "twisted amides", even in cases where a full description of their bonding may be more complex.[3] As such, we focus our discussion specifically on the C(acyl)–N unit undergoing reaction. We briefly introduce classical approaches for C(acyl)–N functionalisation before focusing on recent developments involving mechanisms unique to the late transition metals. For an exhaustive summary of catalytic C(acyl)–N functionalisation reactions, we direct the reader to several reviews focusing on synthetic aspects of these catalytic strategies[3–6] and on transition metal-catalysed activation of C–N bonds more generally.[7,8] While we acknowledge pivotal reports of synthetic methodologies, our discussion prioritizes works providing concrete experimental and/or computational mechanistic insights. As such, the discussion is organized around general mechanistic manifold, including redox-neutral mechanisms, $2e^-$ redox-cycling mechanisms, and mechanisms involving $1e^-$ redox steps. Specifically, we focus on reactions that directly involve a transition metal mediator/catalyst in the C(acyl)–N cleavage step. We conclude with an outlook on the outstanding ambiguities and opportunities for innovation. It is our hope that this Perspective article will spur continued mechanistic investigation to inform the development of increasingly efficient and versatile strategies for transition-metal-catalysed C(acyl)–N functionalisation.

C. Rose Kennedy

C. Rose Kennedy is currently the James P. Wilmot Distinguished Assistant Professor of Chemistry at the University of Rochester. Previously, Rose earned her PhD from Harvard University (2017), working with Professor Eric Jacobsen on enantioselective, ion-binding organocatalysis. She subsequently conducted postdoctoral research with Professor Paul Chirik at Princeton University (2017–2019), where she developed iron-catalyzed methods for the elaboration of simple hydrocarbons. In 2020, Rose began her independent career at the University of Rochester, where her research group uses mechanistic analysis and bioinspired design principles to guide the development of catalytic methods with terrestrially abundant elements. Rose has been recognized with awards including a Packard Fellowship, NIH Maximizing Investigator Research Award, NSF CAREER Award, Kavli Fellowship, Thieme Chemistry Journals Award, and ACS Division of Organic Chemistry Young Investigator Award.

2. Classical mechanisms for amide functionalisation

Most classical mechanisms for functionalisation of amides rely on nucleophilic acyl substitution strategies. However, as the least thermodynamically and kinetically activated carboxylic acid derivatives, amides typically require activation by strong Brønsted or Lewis acids coupled with prolonged reaction times at elevated temperatures (Scheme 1A). Depending on the nature of the N leaving group, this may involve either (a) nucleophile attack first to generate a tetrahedral intermediate (*i.e.* $B_{Ac}2$ or $A_{Ac}2$ mechanisms), or (b) nucleofuge departure first to generate an acylium (or ketene) intermediate (*i.e.* S_N1 mechanism).[9]

Many modern approaches have devised stereoelectronic activating strategies that allow these acyl substitutions to proceed under milder conditions.[10] Building on robust foundational work with bridged, bicyclic lactams,[11] Szostak and co-workers have played a pioneering role in development of acyclic twisted amides that are amenable to both catalytic and uncatalysed acyl substitution protocols (Scheme 1B).[12,13] They have further implemented a combination of spectroscopic

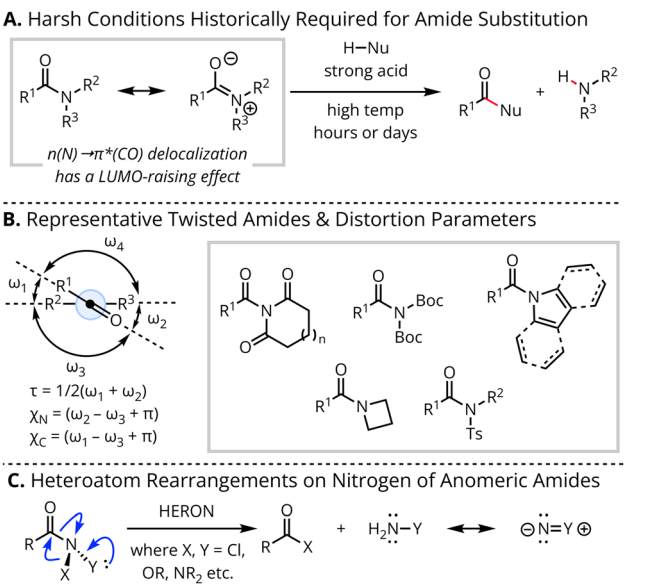

Scheme 1 Approaches for stereoelectronic activation of C(acyl)–N derivatives.

measurements and computational parameterization to benchmark the relative π-electrophilicities of these amide derivatives.[14–18]

In a conceptually related approach, heteroatom rearrangements on nitrogen (HERON) are well-documented when amidic nitrogens are directly connected to two electronegative heteroatoms (Scheme 1C).[19–24] The ensuing rearrangements of these "anomeric amides" have received a resurgence of interest for generation of reactive isodiazenes in the context of N-deletion for skeletal editing applications.[25–28]

The twisted and anomeric amide approaches typically rely on modification of the N nucleofuge. Alternatively, installation of stereoelectronic activating groups on the acyl unit can enhance acyl transfer reactivity. In one such example, Bao and coworkers coupled Cu-catalysed aerobic C–H oxygenation alpha to the carbonyl with subsequent Lewis acid-mediated transamidation.[29] Although this approach involves transition metal catalysis to generate a reactive carboxamide intermediate, the metal does not appear to play any direct role in C(acyl)–N functionalisation of the transient electrophile.

Taken together, these examples highlight both the scope and limitations of uncatalysed C(acyl)–N functionalisation strategies. While transition metal catalysis offers increased mechanistic versatility, strategies for stereoelectronic carboxamide activation—originally developed in the context of purely organic reactions—are generalizable.

3. Redox neutral mechanisms

In analogy to the nucleophilic acyl substitution mechanism, transition metals can deliver organometallic nucleophiles through a redox-neutral or addition–elimination mechanism. This concept has been examined most thoroughly in the context of amide hydrogenation, where chemoselectivity for C–N *vs.* C–O scission remains a defining challenge.[30,31] In its simplest form, elimination would be dictated by the relative rates for elimination of β-H (in the reverse of an initial M–H insertion step), N, and O (Scheme 2).[32–35] However, this model is incomplete as protodemetallation and collapse of a purported hemiaminal intermediate introduces distinct selectivity preferences. An intrinsic reactivity bias favouring expulsion of water poses a substantial challenge in achieving selective C–N scission, which would be attractive for fine chemical synthesis and CO_x capture and valorisation applications. Nonetheless, late transition metals bearing pincer-type ligands have shown promising results favouring C–N bond cleavage. Intriguing mechanistic observations suggest metal–ligand cooperativity or outer-sphere proton delivery as key chemoselectivity-determining factors. These findings thus indicate that it is essential to consider features beyond the primary coordination sphere.

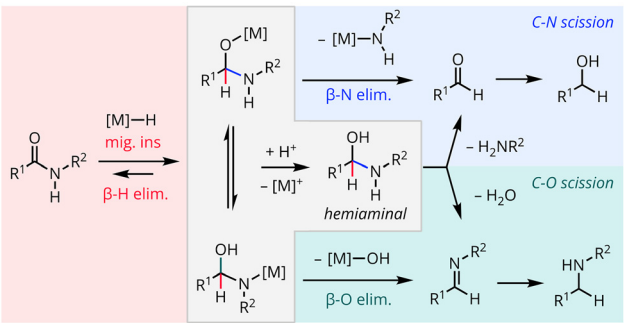

Scheme 2 General model for chemoselectivity in amide hydrogenation controlled by relative rates for elimination from metal-bound and hemiaminal intermediates.

Milstein and coworkers have developed a series of PNN pincer ruthenium(II) complexes (such as **Ru-1** and **Ru-2**, where **Ru-2** is the superior precatalyst) for hydrogenolysis of amides, including the first report of selective C–N scission (Scheme 3A).[36] This reaction is fully reversible, and **Ru-1** also catalyses the dehydrogenative coupling of alcohols with amines to form amides with liberation of H_2.[37,38] Based on established hydrogenation reactivity toward other carbonyl-containing substrates by related catalysts, a mechanism was proposed involving metal–ligand cooperation with aromatization–dearomatization of the heteroaromatic pincer core participating both in (i) heterolytic dihydrogen activation and (ii) substrate organization during metal hydride delivery and hemiaminal breakdown (Scheme 3B).[36] Computational studies from Cantillo in 2011 provided support for the feasibility of such a mechanism with **Ru-2**, albeit with unexpectedly high barriers for both the computed C–O (+52.2 kcal mol^{-1}) and C–N (+51.0 kcal mol^{-1}) scission pathways.[39] Several additional computational studies on the microscopic reverse reaction, dehydrogenative coupling of alcohols and amines to generate amides, reached related conclusions on the role of metal–ligand cooperation in a bifunctional, double-hydrogen-transfer mechanism.[40–42] However, there was some disagreement on the specific mode of metal–ligand cooperation proposed, with Lei, Liu, Schaefer, and coworkers highlighting potential cooperative involvement of an additional unit of alcohol substrate.[43]

Since Milstein's initial report, numerous follow-up works have evaluated other metals, pincer ligands, and variations in reaction temperatures and pressures, enabling development of highly efficient catalysts demonstrating thousands of turnovers in only a few hours.[44–59] Through kinetic profiling and independent synthesis of catalytically active intermediates in the context of analogous ester hydrogenation reactions, Chianese and coworkers demonstrated that the tertiary amine PNN^{Et2} ligands utilised in early reports (as in **Ru-1**) actually undergo hydrodealkylation to generate the corresponding secondary amine PNN^{EtH} ligand (as in **Ru-4**) before entering the catalytic cycle (Scheme 3C).[60,61] Khaskin, Gusev, and coworkers showed that bipyridine-type PNN ligands (as in **Ru-2**) similarly undergo hydrogenation to afford Noyori-type amido complexes **Ru-5** and **Ru-6** under typical hydrogenative (and dehydrogenative) reaction conditions (Scheme 3D).[62] Accordingly, modifying the PNN pincer arm from a pyridyl or tertiary amine group to a secondary amine (as in **Ru-7**) enabled ruthenium-catalysed

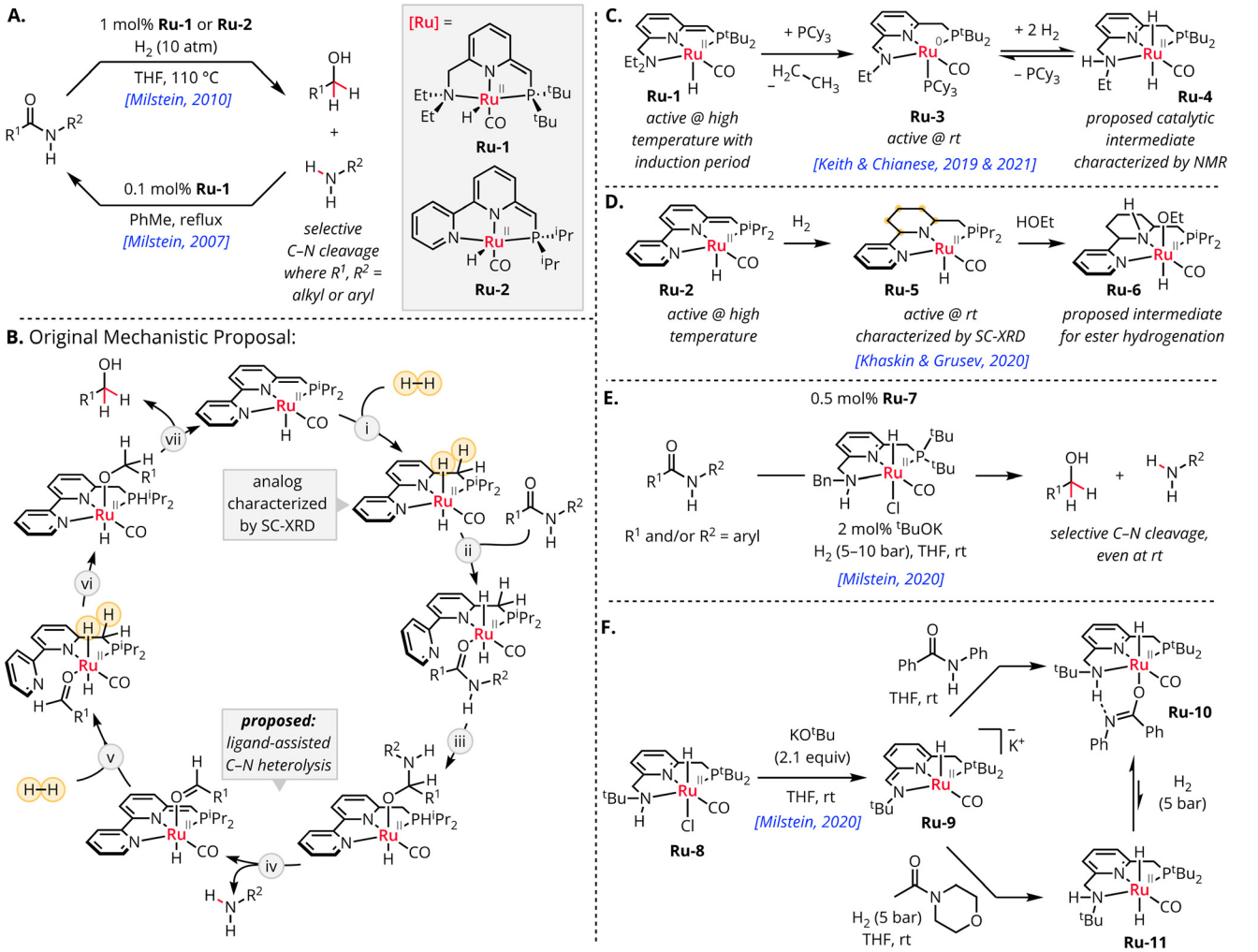

Scheme 3 Development of PNN pincer ruthenium complexes for hydrogenolysis of amides.

amide hydrogenation at lower temperatures and pressures (rt – 45 °C, 5–10 bar H_2 *vs.* 100–150 °C, 10–100 bar H_2) (Scheme 3E).[63]

Deliberate application of these secondary amine PNN complexes under basic conditions revealed formation of an unconventional dearomatized ligand tautomer. In contrast to deprotonation adjacent to the pincer phosphine arm, which had been characterized previously with tertiary amine PNN^{Et2} complexes, the secondary amine PNN^{HEt} complexes instead formed a doubly deprotonated enamido ligand tautomer (**Ru-9**, Scheme 3F).[63] From this anionic, dearomatized intermediate, proton transfer between secondary amide substrates and the enamido ligand enabled off-cycle formation of an unusual κ^1-O coordinated amidate, organized by H-bonding interactions with the ligand (**Ru-10**).[63] When this complex was treated with H_2, a dihydride complex (**Ru-11**) was formed. Upon monitoring by ^{1}H NMR, only amidate complex **Ru-10** (not the dihydride) was observed under catalytic conditions with a secondary amide substrates. With tertiary amide substrates, dihydride complex **Ru-11** was instead observed as the resting state.[63] The persistence of **Ru-11** in this case thus suggested that initial reaction of the amide substrate *via* M–H insertion was the rate-determining step but did not afford any insights into chemoselectivity-determining features.

Follow-up density functional theory (DFT) studies examined the role of secondary amine PNN^{HR} ruthenium complexes in mediating breakdown of the hemiacetal and hemiaminal intermediates formed in ester and amide hydrogenolysis reactions, respectively, with conflicting results.[61,64] The lowest barrier pathway identified in the absence of explicit solvent involved H-bonding or proton-transfer from the backbone CH_2 to the departing N nucleofuge (Scheme 4A).[64] By contrast, inclusion of explicit ethanol solvation enabled identification of a more energetically reasonable pathway involving proton transfer from the PNN secondary amine sidearm to a departing O nucleofuge (Scheme 4B).[61] Additional investigation is necessary to assess whether a similar pathway may be operative for hemiaminal breakdown.

While additional follow-up studies are clearly needed to resolve the competing mechanistic proposals for hemiaminal

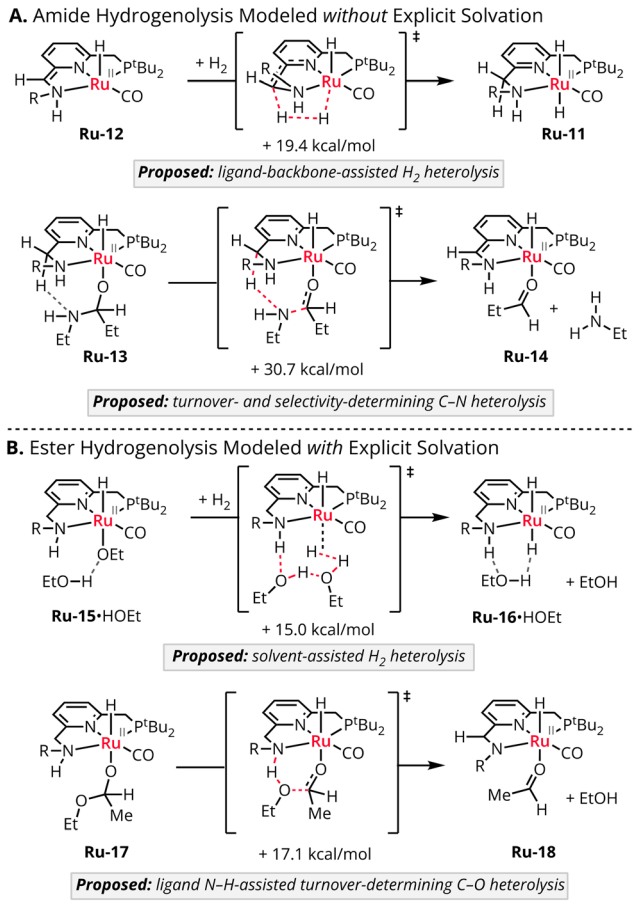

Scheme 4 Competing mechanistic proposals from computational studies of secondary amine PNN Ru catalysts for hydrogenolysis of amides and esters.

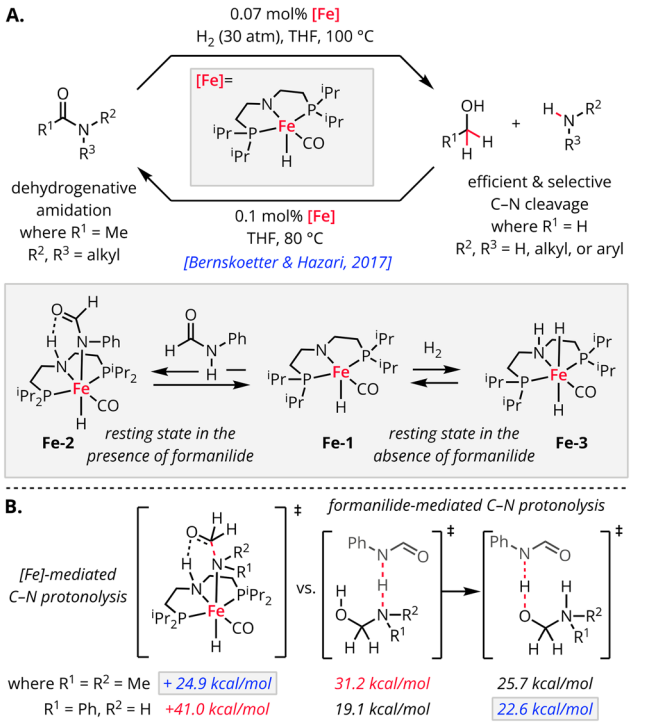

Scheme 5 PNP iron catalysed amide hydrogenolysis and substrate-dependent mechanisms for hemiaminal C–N protonolysis in a key chemoselectivity-determining step.

breakdown with PNN Ru complexes,[65] substantial progress has been made toward the development and understanding of related pincer iron complexes as catalysts for hydrogenation of amides, esters, and CO_2.[66,67] Contemporaneous reports from the Langer[51] and Bernskoetter/Hazari groups[53,68] in 2016–2017 described Noyori-type iron complexes such as [(^{iPr}PN^{H}P)Fe(H)$_2$(CO)] (**Fe-1**, where ^{iPr}PN^{H}P = HN(CH$_2$CH$_2$(P^{i}Pr$_2$))$_2$) for deaminative hydrogenolysis (C–N scission) of varied formamides with impressive initial rates and turnover numbers (TONs > 1000 in 3 hours at 100 °C, 30 atm H_2) (Scheme 5A). Perplexingly, secondary formamide additives were required for most efficient reactivity of tertiary formamides.[53]

In 2018, Bernskoetter, Hazari, Nova and co-workers disclosed a follow-up study focusing on the mechanism of deaminative hydrogenation and the basis for this unusual additive effect with the ^{iPr}PN^{H}P iron system.[69] Based on density functional theory (DFT) calculations and microkinetic modelling, they validated the intermediacy of hemiaminals formed from near-thermoneutral insertion into the metal hydride. However, the mechanism for hemiaminal breakdown varied across substrates, where the lowest-barrier pathway for formanilide involved cooperative proton transfer and stabilization of the incipient iron amido during a concerted outer-sphere elimination (Scheme 5B). However, for *N*,*N*-dimethylformamide, the corresponding iron-mediated aminolysis step was instead kinetically prohibitive as a stepwise process. Based on this observation, the authors invoked a co-catalytic role for the secondary formamide additive in assisting with the final elimination step without the involvement of iron (Scheme 5B). This finding was particularly significant because it challenged the conventional assumption that hydrogenation reactivity toward electron-rich carboxylic acid-derivatives was limited exclusively by the metal-hydride hydricity. Furthermore, this mechanistic insight was extended to the rational development of an optimized guanidine co-catalyst (triazabicyclodecene, TBD) that maximized rates of proton transfer while minimizing catalyst poisoning and other decomposition processes.[70,71]

Although the examples of amide hydrogenation catalysts discussed above all involve pincer metal complexes, substantial opportunity for innovation beyond this catalyst space remains. As a highlight, in 2022, Razayee and coworkers disclosed a distinct, 1,10-phenanthroline-2,9-diol-supported iridium catalyst system (**Ir-1**) capable of achieving switchable C–O and C–N scission of carboxamides (Scheme 6).[72] Under acidic conditions, exclusive C–O scission was observed. However, when a base was introduced into the hydrogenation process, chemoselectivity switched to favour C–N scission instead. The proximity of the ligand protic site near the metal further proved crucial for this C–N activation. The researchers hypothesized that these catalysts may rely on a distinct

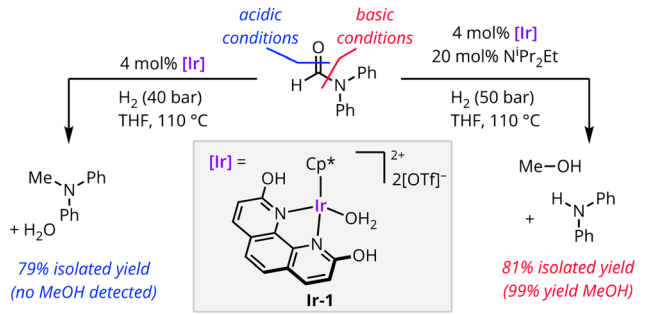

Scheme 6 Ir-catalysed amide hydrogenolysis with switchable chemoselectivity.

mode of metal–ligand-cooperativity for H_2 heterolysis and/or substrate activation. As such, additional mechanistic work is needed to distinguish the potentially generalizable, chemoselectivity-determining features defined by this distinct catalyst system.

4. 2e⁻ redox-cycling mechanisms

Perhaps the most widely appreciated motivation for pursuing transition metal catalysis is the opportunity to achieve transformations with no direct organic counterparts through multielectron redox changes. As such, it is logical that 2e⁻ redox-cycling mechanisms, especially Ni(0/II) and Pd(0/II) catalytic cycles, are most commonly invoked for non-hydrogenative C(acyl)–N functionalisation. The typical proposed mechanism for a M(0/II) cycle begins with oxidative addition of the electrophile into the M(0) catalyst (step i), resulting in the formation of an acyl metal intermediate (Scheme 7). This intermediate undergoes transmetallation (step ii) with a nucleophile, and subsequent reductive elimination (step iii) yields the carbonyl-retentive product. Alternatively, CO deinsertion (step ii′) prior to reductive elimination (step v′) would afford the decarbonylated product. Slight variations involving transmetallation prior to oxidative addition are also possible.

In 2015, the Szostak and Zou groups independently reported the first examples of palladium-catalysed cross-coupling reactions between twisted amides and boronic acids to yield carbonyl-retentive ketone products (Scheme 8A and B).[73,74] Both reports included mechanistic proposals involving Pd(0)-mediated oxidative addition into the substrate C(acyl)–N bond, where substrate conversion (and product yield) correlated with the degree of ground-state C(O)–N distortion. Additionally, Szostak and coworkers detected mono- and bis-phosphine-supported palladium acyl and aryl species through electrospray ionization mass spectrometry (ESI/MS) analysis.[74] These findings provided supporting evidence that amide C(acyl)–N bond activation followed an oxidative addition pathway in this case.

In the same year, the Garg group reported the first Ni-catalysed C(acyl)–N functionalisation of amides.[75] Utilizing the electron-rich SIPr/Ni system (SIPr = 1,3-bis(2,6-di-isopropylphenyl)imidazolidin-2-ylidene), Garg and coworkers successfully carried out esterification of weakly activated *N*-methylbenzanilide (Scheme 8C). Based on evaluation of the reaction coordinate diagram using DFT, they also proposed oxidative addition to be the rate-determining step in the reaction.[75] A follow-up kinetic modelling study examined the esterification of *N*-methyl-benzanilide with (−)-menthol and found that the kinetic data could be fitted to a series of steps agreeing with this computational model. This study also identified a competitive unknown pathway for catalyst degradation.[76]

Following these pivotal early demonstrations, there have been numerous reports of Ni[77–104] and Pd[73,95,105–114] and (to a

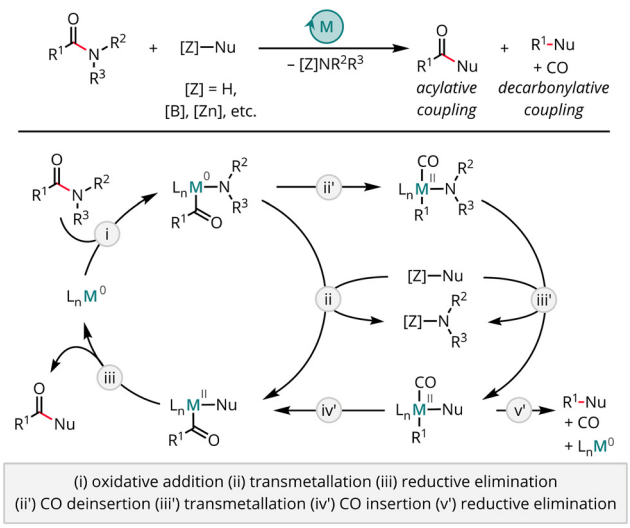

Scheme 7 General 2e⁻ redox-cycling mechanism proposed for acylative and decarbonylative coupling reactions with C(acyl)–N electrophiles. Nu = nucleophile.

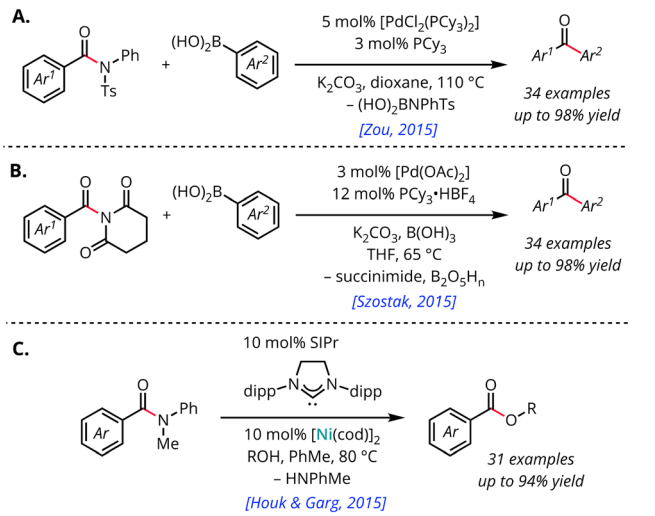

Scheme 8 Key early developments in Pd- and Ni-catalysed acylative coupling using C(acyl)–N electrophiles. Ar = aryl; cod = 1,5-cyclooctadiene; dipp = 2,6-diisopropylphenyl; Ts = 4-toluenesulfonyl.

lesser extent) other metal-catalysed[115–119] methods for acylative and decarbonylative functionalisation of amides.[2,109,120] However, despite these synthetic developments, mechanistic studies, especially *experimental* mechanistic studies, have been comparatively limited.

4.1 Experimental mechanistic studies with Ni

The first report providing experimental evidence for the accessibility of Ni(II) species by C(acyl)–N bond activation in amides was reported by Shi and coworkers in 2016.[93] They reported a decarbonylative borylation of amides using $Ni(OAc)_2{\cdot}2H_2O$ and ICy·HCl (ICy = 1,3-dicyclohexylimidazolidene) to generate the active catalyst *in situ*.[93] Through stoichiometric studies using $[Ni(cod)_2]$ in place of $Ni(OAc)_2{\cdot}2H_2O$, they successfully isolated a bis(NHC)-supported Ni(II) acyl species (**Ni-1**), which underwent decarbonylation to form the corresponding Ni(II) aryl (**Ni-2**) upon heating (Scheme 9A). Subsequent treatment of **Ni-2** with B_2nep_2 (nep = neopentyl glycolato) resulted in the formation of the desired borylated product, thereby confirming the decarbonylated species as an intermediate in the reaction. Both **Ni-1** and **Ni-2** were fully characterized by SC-XRD, and **Ni-1** proved to be an effective catalyst for the net borylation, further supporting the catalytic relevance of the isolated species.

Soon thereafter in 2017, Lahiri, Maiti, and coworkers reported detection by ESI-MS of cod-supported Ni(II) acyl species (**Ni-3** and **Ni-4**) in the context of a phosphine/Ni-catalysed deamidative reduction of *N*-acyl pyrazoles (Scheme 9B).[121] The authors also validated the formation of $Ni(CO)_n(EtPPh_2)_2$ (**Ni-6**) by IR spectroscopy and SC-XRD and demonstrated that the $Ni(CO)_n(EtPPh_2)_2$ adducts were chemically competent for the reductive transformation at high temperatures (130 °C).

In 2023, both the Kennedy[122] and Morandi[123] labs independently reported further mechanistic organometallic work using single-component [Ni(SIPr)(benzene)] (**Ni-7**) and [Ni(IPr)(toluene)] (**Ni-11**) precatalysts, respectively. Kennedy and coworkers evaluated both the accessibility and catalytic activity of Ni(0), Ni(I) nucleophile (**Ni-8**), and Ni(II) acyl (**Ni-9** and **Ni-10**) complexes (Scheme 10A).[122] They demonstrated that carbamate activating groups played key roles in both the kinetic accessibility and thermodynamics of C(acyl)–N oxidative addition at Ni(0), where the carbamate acts as a chelating ligand to stabilize the Ni(II) acyl (**Ni-9** or **Ni-10**) and inhibit CO-deinsertion. Based on a double-labelling crossover experiment, Kennedy and coworkers also provided the first experimental evidence for the kinetic accessibility of C(acyl)–N oxidative addition with relatively unactivated amides such as *N*-methylbenzanilide, where the corresponding Ni(II) acyl lies energetically uphill (K_{eq} < 1, Scheme 10B). Finally, they demonstrated that Ni(I) species are formed under catalytically relevant conditions through comporoportionation of **Ni-7** and **Ni-9**. This process represented a primary catalyst deactivation pathway where the Ni(I) adducts afforded reduced or no catalytic activity (depending on the amide) and counterproductive chemoselectivity favouring cleavage of carbamoyl activating groups. As such, this work provided molecular-level insight into the catalyst deactivation processes noted previously and suggested that single-component precatalysts avoiding inefficient *in situ* activation could enable the use of lower catalyst loadings that would circumvent this challenge.

Morandi and coworkers demonstrated analogous C(acyl)–N oxidative addition with carbamate-activated aliphatic lactams.[123] As noted by the Kennedy team, Morandi and coworkers found that the carbamate acted as a chelating group to stabilize the resulting Ni(II) acyl metallacycles (**Ni-12** and **N-14**). However, they found that metallacycle ring-size and -strain, presumably controlling the geometry of carbamate chelation, gated the accessibility of decarbonylation (Scheme 10C). With 7-membered (from δ-lactams) and larger acyl nickelacycles (such as **Ni-14**), CO deinsertion and dissociation proceeded readily at room temperature. By contrast, CO deinsertion and dissociation from 6-membered acyl nickelacycles (such as **Ni-12**, from γ-lactams) proceeded slowly over multiple days and not at all from the corresponding 5-membered acyl nickelacycles (from β-lactams).

In complementary work, Stanley and coworkers reported the Ni-catalysed intramolecular carboacylation of alkenes *via*

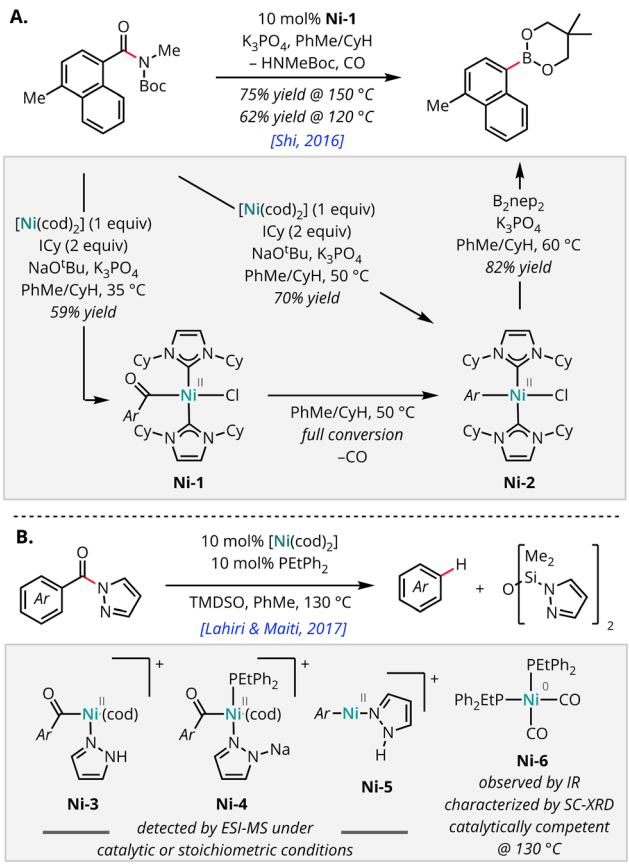

Scheme 9 Experimental evidence for Ni(0/II) oxidative addition into C(acyl)–N electrophiles relevant to decarbonylative functionalisation reactions. Ar = aryl; cod = 1,5-cyclooctadiene; ICy = 1,3-dicyclohexylimidazol-2-ylidene; nep = neopentyl glycolato; TMDSO = 1,1,3,3-tetramethyldisiloxane.

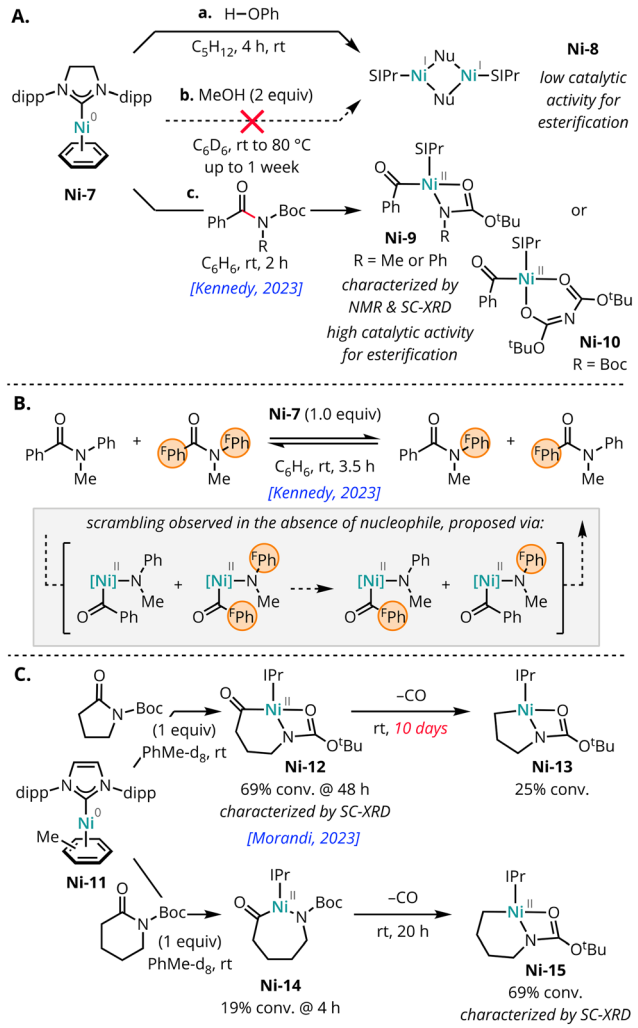

Scheme 10 Experimental evidence for Ni(0/II) oxidative addition into C(acyl)–N electrophiles relevant to acylative functionalisation reactions. Ar = aryl; Ar^F = 4-fluorophenyl; Boc = *tert*-butoxycarbonyl; cod = 1,5-cyclooctadiene; dipp = 2,6-diisopropylphenyl; IPr = 1,3-bis(2,6-di-isopropylphenyl)imidazol-2-ylidene; SIPr = 1,3-bis(2,6-di-isopropylphenyl)imidazolidin-2-ylidene.

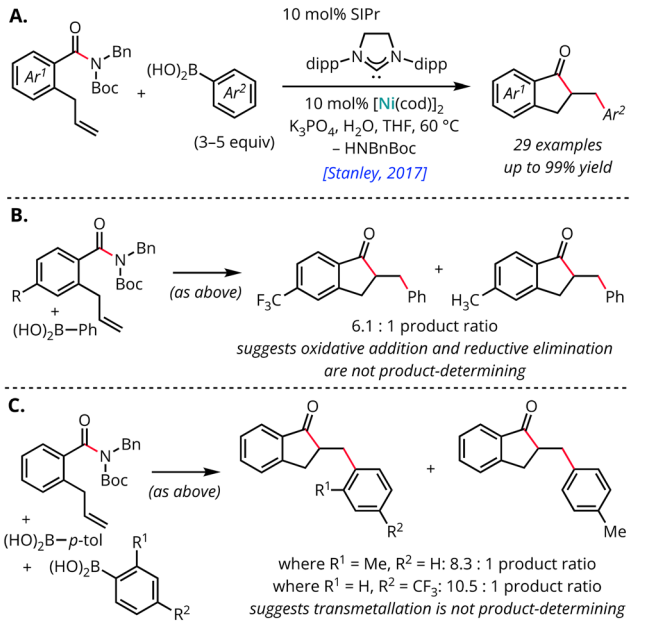

Scheme 11 Competition experiments evaluating Ni-catalysed intramolecular carboacylation of alkenes by C(acyl)–N functionalisation. Ar = aryl; Boc = *tert*-butoxycarbonyl; cod = 1,5-cyclooctadiene; dipp = 2,6-diisopropylphenyl; IPr = 1,3-bis(2,6-di-isopropylphenyl)imidazol-2-ylidene; SIPr = 1,3-bis(2,6-di-isopropylphenyl)imidazolidin-2-ylidene.

C(acyl)–N activation of amides (Scheme 11A).[88] Shortly thereafter, the same group reported a 3-component variant using norbornenes as the alkene component.[89] These reactions constitute examples of conjunctive (rather than direct) cross-coupling with C(acyl)–N electrophiles.[124] In both cases, the authors performed several competition experiments to evaluate the nature of the product-determining steps and the plausible sequences of migratory insertion and transmetallation. Competition experiments between electron-rich and electron-deficient amides yielded a preference for product formation from the electron-deficient amide (Scheme 11B). Electron-rich species have been shown to favour oxidative addition by decreasing C=N character;[18] however, the arene electronics should have no impact on the rate of distal C–C reductive elimination. Taken together, this result led the authors to conclude that neither oxidative addition nor reductive elimination was rate- or product-determining. Interestingly, in the case of intramolecular carboacylation, they observed that ketones derived from electron-deficient and sterically hindered aryl boron nucleophiles exhibited higher yields than their more nucleophilic electron-rich, unhindered counterparts (Scheme 11C).[88] This observation suggested that transmetallation also was not rate-determining. However, the use of even stronger Ph_2Zn nucleophiles led to the formation of direct acylative Suzuki–Miyara coupling products,[89] suggesting that transmetallation must follow (rather than precede) migratory insertion. By process of elimination, the author's concluded that migratory insertion was most likely the rate-determining step for intramolecular carboacylation.[88] However the observations may also be consistent with rate- and product-determining reductive elimination, as was concluded for the 3-component carboacylation.[89]

4.2 Computational mechanistic studies with Ni

Beginning from the earliest reports of metal-catalysed cross-coupling with twisted-amide electrophiles, computational studies have played a key role in rationalizing general reactivity and chemoselectivity trends.[125] Building from Houk and co-workers' initial examination of Ni-catalysed esterification of amides,[75] a series of papers from the Zhao,[126] Fu,[127] and Hong[128] groups in 2016 and 2017 addressed Ni-catalysed Suzuki–Miyaura couplings using *N*-benzoyl carbamates[126,127] and glutarimindes[128] as electrophiles, respectively. Generally, these studies only addressed the feasibility of $2e^-$ redox-

cycling mechanisms, although redox-neutral mechanistic proposals may also be viable in some cases.

Zhu, Zhao, and coworkers revealed that the chemoselectivity of oxidative addition into *N*-benzyl-*N*-*tert*-butoxycarbonyl (*N*-Bn-*N*-Boc) benzamide is under thermodynamic control with the SIPr/Ni catalyst system (Scheme 12A).[126] Although oxidative addition of Ni(0) into the C(acyl)–N and C(carbamoyl)–N bonds share similar activation barriers, the product of C(acyl)–N oxidative addition is nearly 10 kcal mol^{-1} more stable, due in part to the favourable chelating ability of the carbamate leaving group.

Hong and coworkers examined the complementary PCy_3/Ni catalyst system, which promoted decarbonylative Suzuki–Miyaura coupling using *N*-acyl glutarimide electrophiles.[128] In contrast to the studies examining the SIPr/Ni catalyst system, they found that chelation of the glutarimide O to Ni substantially lowered the barrier for oxidative addition in addition to stabilizing the resulting Ni(II) acyl complex (Scheme 12B). They noted a similar, albeit higher energy, pathway with the analogous benzoyl carbamates as well. Additionally, they examined the origin of chemoselectivity for decarbonylated *vs.* carbonyl-retentive products. As in prior studies, they noted that the barrier for carbonyl-retentive reductive elimination was lower than that of CO deinsertion, rendering the carbonyl-retentive ketone the kinetically preferred product for reactions with strong nucleophiles at moderate temperatures. However, for reactions requiring higher temperatures to achieve transmetallation, the ketone could be activated to allow access to the thermodynamically-favoured decarbonylative product. Their computational findings were validated by a contemporaneous report from Tobisu, Chatani, and coworkers on the nickel-mediated decarbonylation of unstrained ketones.[129]

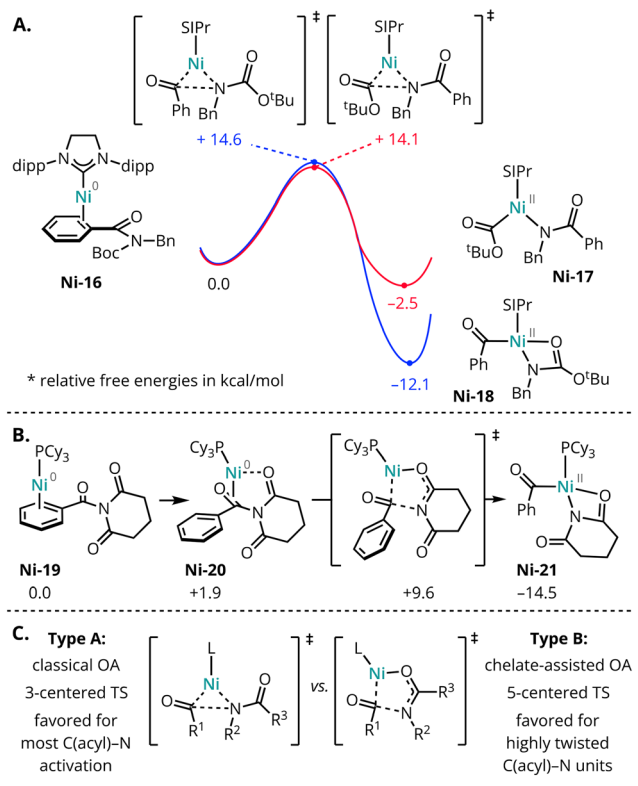

Scheme 12 Computational modelling of Ni(0)-mediated C(acyl)–N oxidative addition. Boc = *tert*-butoxycarbonyl; dipp = 2,6-diisopropylphenyl; OA = oxidative addition; SIPr = 1,3-bis(2,6-di-isopropylphenyl) imidazolidin-2-ylidene; TS = transition state.

In 2018, the Dang group reported a theoretical study comparing the esterification of α-aryl and α-alkyl amides,[130] which required different ligand designs in their development.[75,79] Dang and coworkers suggested that a 2e$^-$ redox-cycling pathway was likely conserved across the different amide and ligand combinations, and rationalized the basis for substrate–ligand matching effects. With α-aryl amides, they proposed that the electron-richness of the SIPr *vs.* terpyridine ligands was responsible for gating the energetic accessibility of the oxidative addition step. Conversely, they noted that the SIPr ligand system resulted in a prohibitively high barrier for proton-transfer between MeOH and NBnBoc during the ligand metathesis step with α-alkyl amides. Building upon these findings, they also computationally proposed that an electron-rich terpyridine ligand bearing multiple dimethylamine groups could carry out esterification of both aryl and alkyl amides. To the best of our knowledge, this prediction has not been tested experimentally.

In summarizing these works, Hong and coworkers noted that, across systems, Ni(0) can interact with acyl and amine fragments through two distinct mechanistic pathways for oxidative addition (Scheme 12C).[125,131] The type A mechanism resembles classical oxidative addition mechanisms through a 3-centered transition state leading to cleavage of the C(acyl)–N bond. In the type B pathway, a coordinating substituent on N can induce chelation-assisted oxidative addition through a larger-membered transition state. In most cases, the stability obtained through chelation does not sufficiently compensate for the energy penalty due to distortion from the 3-membered transition state. As a result, the type A mechanisms are generally preferred, even for substrates bearing a chelating group. As such, the chelation of carbamate activating groups noted by Kennedy[122] and Morandi[123] reflects primarily product- rather than transition-state stabilization. By contrast, substrates that are highly twisted from planarity in their ground states (such as *N*-acyl glutarimides) avoid this energetic penalty when proceeding through the type B, chelate-assisted oxidative addition. Regardless of mechanistic manifold, the primary factor responsible for the cleavage of the C(acyl)–N bond is the π coordination of Ni to the acyl fragment, which further weakens $n_N \rightarrow \pi^*_{CO}$ delocalisation, and the barrier for oxidative addition can be correlated with the heterolytic bond strength (pK_a) of the corresponding leaving group.

4.3 Mechanistic studies with other metals

Though much of the reported work involves palladium and nickel, there have also been reports on amide C–N activation using several other metals as catalysts. However, the mechanistic studies using these metals have been limited. The first

rhodium-catalysed acyl C–N bond activation was reported by the Szostak group in 2016 using the $[Rh(cod)Cl]_2$ system (Scheme 13A).[115] This work featured directed C–H arylation of pyridyl arenes using *N*-acyl glutarimides as the electrophilic coupling partners. Using ESI-MS analysis of reactions conducted with stoichiometric mixtures of [Rh], base, and amide, the authors detected formation of rhodium aryl intermediates (such as **Rh-1**), consistent with oxidative addition of the C–N bond of the amide to the Rh(I) catalyst, accompanied by elimination of CO.

The first cobalt-catalysed amide C–N bond activation was reported by Gosmini, Danoun, and coworkers in 2017, wherein $CoBr_2$ in combination with bipyridine and TMSCl-activated manganese catalysed the esterification *N*-Boc with primary and secondary alcohols.[118] Even though a deep mechanistic understanding of this reaction has yet to be revealed, they proposed a possible mechanism that proceeds *via* the oxidative addition of the acyl C–N bond of the amide substrate into a Co(0) catalyst generated *in situ*.

In 2021, Zhang, Bao, and coworkers reported the first ruthenium catalyst for the C(acyl)–N bond activation of amides (Scheme 13B).[119] Using $[RuCl_2(p\text{-cymene})_2]$ as a precatalyst in combination with K_2CO_3 and 2,4,6-triisopropylbenzoic acid additives, they developed methodology for C–H acylation of 2-arylpyridines using *N*-phenyl-*N*-tosylamides as acylating agents. Based on the absence of an H-atom kinetic isotope effect in competition experiments, they concluded that C–H activation was unlikely to be rate-determining. Cycloruthenated complex **Ru-19** was found to be an effective catalyst, but only in the presence of additional 2-arylpyridine. Based on this observation, the authors proposed that a biscycloruthenated complex **Ru-20** was responsible for C(acyl)–N activation in the rate-determining step (Scheme 13C).

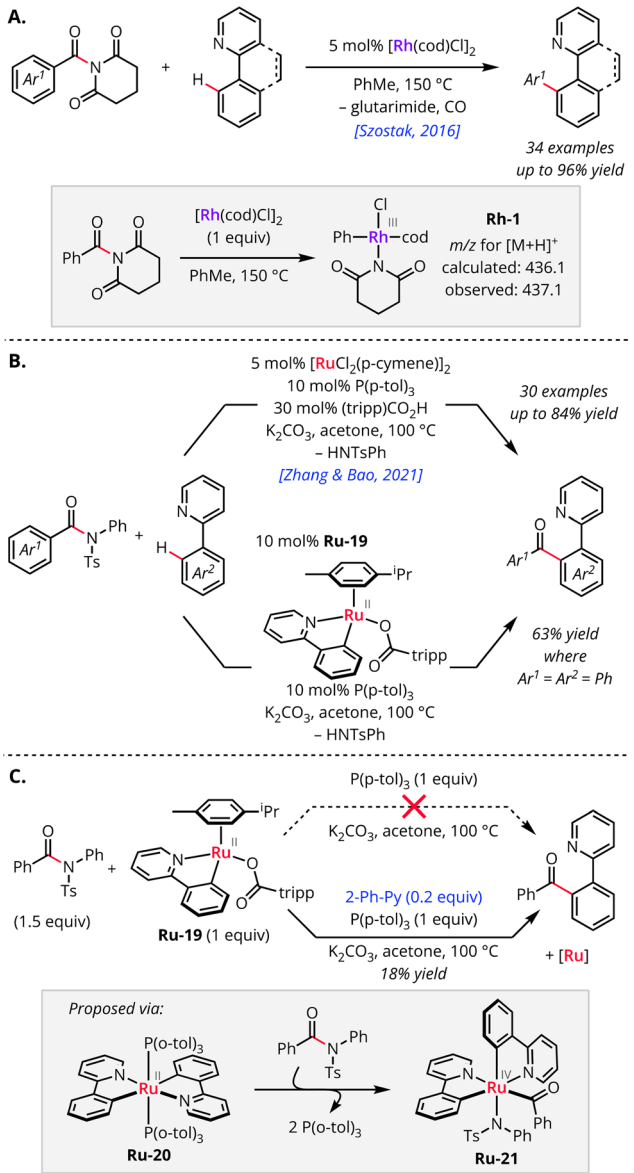

Scheme 13 Catalytic application on C(acyl)–N activation using metals other than Pd and Ni with evidence for $2e^-$ redox-cycling mechanisms. Ar = aryl; cod = 1,5-cyclooctadiene; tol = toluyl = 4-methylphenyl; tripp = 2,4,6-triisopropylphenyl; Ts = 4-toluenesulfonyl.

4.4 Outstanding mechanistic questions

Taken together, these works hint at the versatile potential of C(acyl)–N functionalisation through $2e^-$ redox-cycling mechanisms but also highlight the many frontiers still to be evaluated. While the mechanistic work from the Szostak, Shi, Maiti, Kennedy, and Morandi labs provided unambiguous evidence for the feasibility of C(acyl)–N oxidative addition at neutral Pd(0)[74] and Ni(0),[93,122,123] the nature of oxidative addition with other metals has been evaluated less extensively. Additionally, even in the context of nickel catalysis, all of the mechanistic studies performed to-date have examined reactions with relatively weak nucleophiles or reactions proceeding in the absence of an exogenous nucleophile altogether. Alternative pathways involving nickelate formation must be considered further, especially in cases involving stronger nucleophiles such as organozinc, organoaluminum, or organomagnesium reagents.[132–134] The resulting metalates may then react either through redox-neutral insertion/elimination-type or $2e^-$ redox-cycling mechanistic manifolds.

Additionally, for reactions involving conjunctive cross-couplings or apparent Heck-type reactions across a π system, the possibility of competing oxidative cyclization manifolds must be considered (Scheme 14).[135,136] Computational studies from Sato and coworkers on a related transformation indicated that oxidative cyclization manifolds were substantially lower in energy than alternatives proceeding through C(acyl)–O oxidative addition.[137] Oxidative cyclization-type mechanisms are also prevalent for [Ni]/NHC-catalysed transformations involving aldehydes[138,139] and α,β-unsaturated esters.[140–142] The intriguing possibilities of tapping alternative mechanisms, with distinct chemoselectivity profiles depending on the specific combinations of reagents merit further study and hold promise for future synthetic innovation.

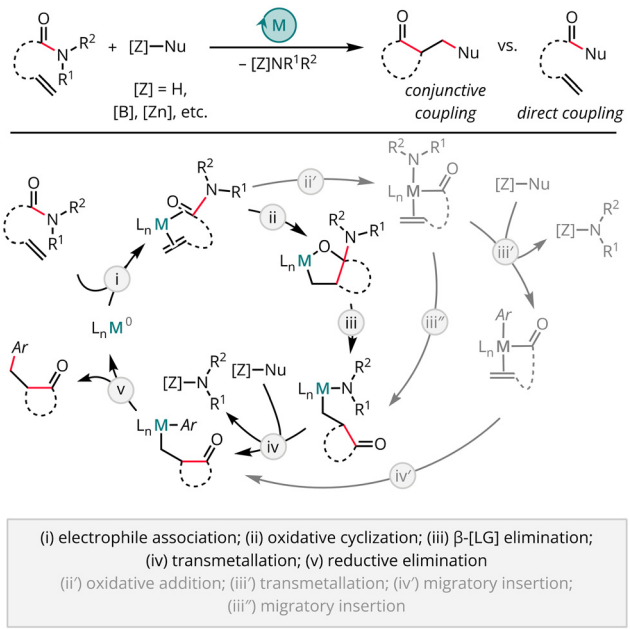

Scheme 14 Alternative mechanistic proposal for conjunctive coupling reactions with C(acyl)–N electrophiles.

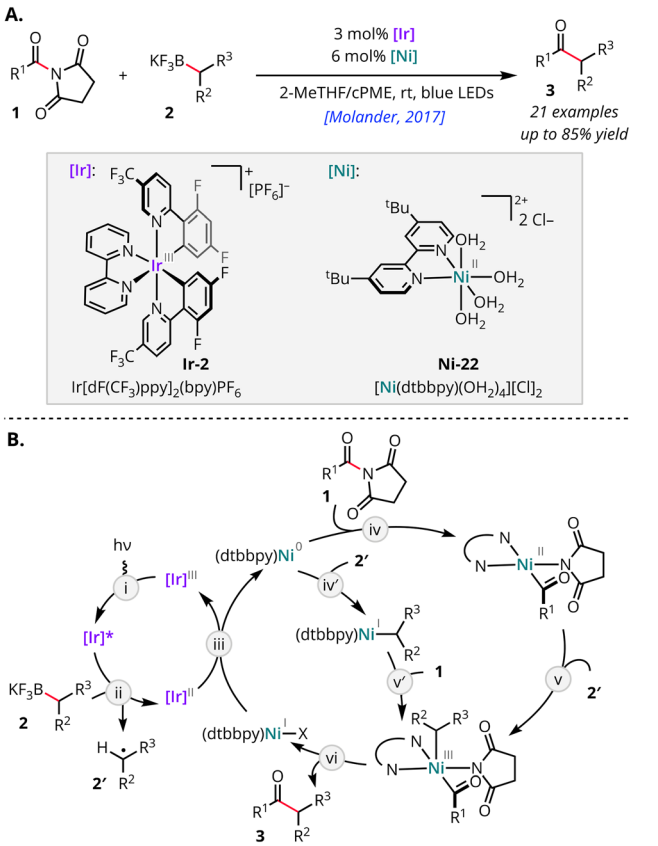

Scheme 15 Key early development in Ni-catalysed acylative coupling using a C(acyl)–N electrophile with dual photoredox and Ni catalysis.

5. 1e⁻ mechanisms

Building on the developments of C(acyl)–N functionalisation by 2e⁻ redox-cycling mechanisms, more complex catalytic mechanisms involving both 2e⁻ and 1e⁻ steps were soon investigated. This work was supported by the surge of interest in reductive cross coupling, metallaphotoredox catalysis, and electrocatalytic organic synthesis. Initial works in this area relied on the Ni(0)-enabled oxidative addition reactivity discussed above,[143,144] but more recently, the potential 1e⁻ reactivity of activated amides has been recognized to provide access to an expanding range of transformations.[145–147]

In 2017, the Molander group reported a dual photoredox and nickel-catalysed acylation of potassium alkyl fluoroborates with *N*-acyl succinimide electrophiles to form aliphatic ketones (Scheme 15A).[143] Although their report did not include any mechanistic experiments, the authors drew on related prior works to propose two plausible mechanistic paths beginning from Ni(0), with simultaneous photoredox-catalyst-enabled oxidative fragmentation of the alkyltrifluoroborate (Scheme 15B, steps i–ii). Sequential C(acyl)–N oxidative addition and alkyl radical capture, in either order, would lead to a common Ni(III) acyl intermediate (steps iv–v or iv′–v′). Reductive elimination (step vi) would form the product and a Ni(I) complex, which was proposed to undergo SET with Ir(II) to regenerate the active Ni(0) species and ground state Ir(III) photocatalyst (step iii).

The same year, Han and coworkers reported a method for reductive cross-coupling of *N*-acyl glutarimides with aryl iodides (Scheme 16A).[144] Based on radical trapping experiments and the observation of Ni acyl species by ESI-MS, the authors proposed a catalytic cycle in which the tpy/Ni(0) (tpy = 2,2′;6′,2″-terpyridine) catalyst selectively undergoes C(acyl)–N oxidative addition (Scheme 16B, step ii) prior to capture of an aryl radical generated through a chain mechanism (step iii). Reductive elimination from the resulting Ni(III) acyl complex (step iv) would form the observed ketone product. Halide abstraction by the resulting Ni(I) would generate additional phenyl radical (step v), and subsequent reduction with Zn(0) (step vi) would regenerate the active Ni(0) species.

In 2020 and 2021, the Baik & Hong groups and the Amgoune group independently reported highly similar methods involving dual photoredox and Ni-catalysed acylation of alkanes with *N*-acyl succinimide electrophiles (Scheme 17A).[145,146] Both groups used Ni(II) salts in combination with dtbbpy (dtbbpy = 4,4′-di-*tert*-butyl-2,2′-dipyridyl) as precatalysts under the assumption that reduced nickel species would be generated *in situ* under the photoredox conditions. Amgoune and coworkers demonstrated through the combination of NMR monitoring and SC-XRD analysis that Ni(II)-acyl and Ni(II)-aryl (**Ni-26**) species formed readily upon treatment of *N*-benzoylsuccinimide with [(dtbbpy)Ni(cod)] (**Ni-25**).[146] However, quite surprisingly, **Ni-25** performed very poorly as a catalyst (yielding only 8% of the desired product), and the isolated Ni(II)-aryl (**Ni-26**) was completely inactive (Scheme 17B). Moreover, more active acyl electrophiles such as benzoyl chlor-

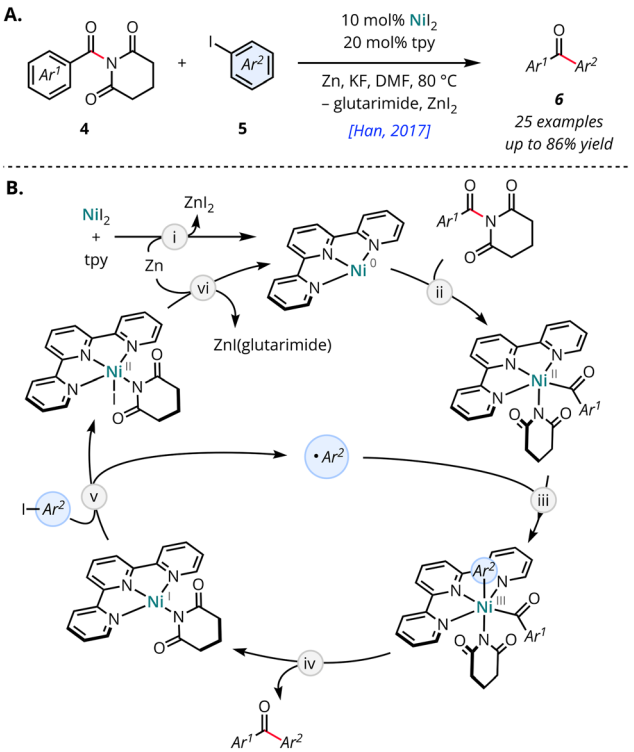

Scheme 16 Key early development in Ni-catalysed reductive acylative cross-coupling using a C(acyl)–N electrophile.

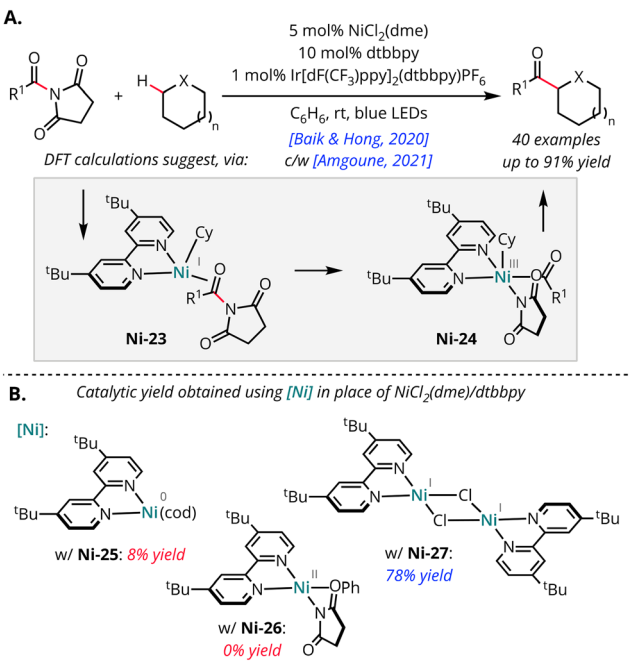

Scheme 17 Ni-catalysed C–H acylation using C(acyl)–N electrophiles.

ide and benzoic anhydride were poor substrates in comparison with *N*-benzoylsuccinimide.[145] These observations suggested that, despite its accessibility, the Ni(0/II) oxidative addition pathway was likely not operative in the overall catalytic transformation. By contrast, Amgoune and coworkers found that a Ni(I) dimer (**Ni-27**) was catalytically active for the reaction and even showed higher efficiency than their original Ni(II) catalyst (Scheme 17B).[146] Baik, Hong, and coworkers supplemented these surprising experimental findings with a detailed computational investigation, which suggested that C–H activation *via* a photoinduced reaction from [(dtbbpy)$NiCl_3$], preceded C(acyl)–N oxidative addition. Following multiple reductions mediated by the photocatalyst, a Ni(I) alkyl complex (**Ni-23**) was proposed to be responsible for the C(acyl)–N oxidative addition to form **Ni-24**, which undergoes facile reductive elimination to form the ketone product.

In a subsequent report, the Amougne and Vantourout groups built on these findings to develop an electro-reductive coupling of *N*-acyl succinimides with alkyl halides using an analogous dtbbpy/nickel catalyst system (Scheme 18A).[147] Through a series of cyclic voltammetry (CV) studies, the authors demonstrated that an electrogenerated Ni(I) species (**Ni-29**) can activate both the alkyl bromide (by SET and alkyl radical formation, Scheme 18B, step ii) and the *N*-acyl imide (by C–N oxidative addition, step iii) electrophiles. The authors proposed that rapid comproportionation of the resulting Ni(III) acyl with remaining **Ni-29** or electroreduction would afford the corresponding Ni(II) acyl (step iv), which could then capture the alkyl radical *en route* to the cross-coupled product (Scheme 18B, steps v–vi).

Taken together, these works challenge key assumptions about catalytically relevant mechanisms of *N*-acyl-imide activation and highlight the importance of evaluating mechanistic assumptions experimentally. They further suggest that a broader range of mechanisms than previously assumed may

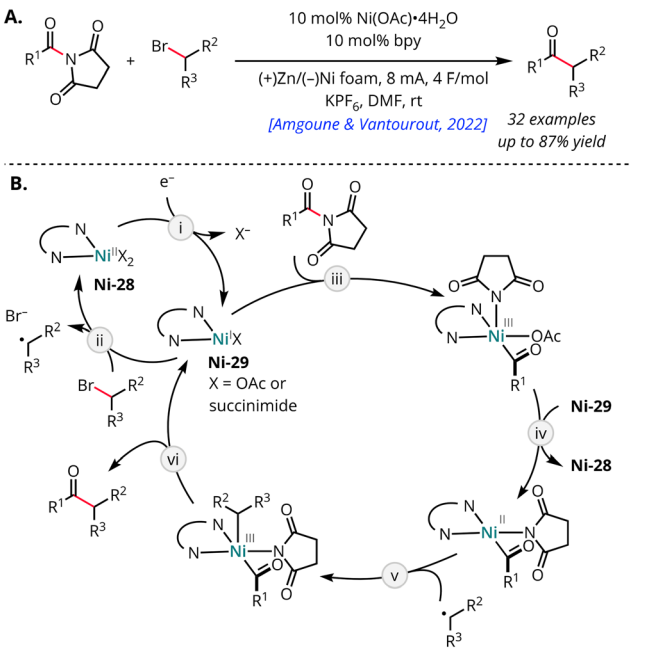

Scheme 18 Ni-catalysed electroreductive coupling using C(acyl)–N electrophiles.

be operative for many of the C(acyl)–N functionalisation reactions developed to date, highlighting opportunities for further innovation within these diverse mechanistic manifolds.

6. Outlook & conclusions

In conclusion, substantial recent work has provided foundational insights into several distinct mechanisms through C(acyl)–N functionalisation through redox-neutral, $2e^-$ redox-cycling, and $1e^-$ mechanisms. These studies hold promise for informing the development of new catalytic methodologies that overcome current limitations to catalytic efficiency and enable entirely new reactivity patterns. However, these studies have only scratched the surface, and many questions remain to be evaluated. The field is ripe for continued synergy of mechanistic study and reaction discovery to push the boundaries of C(acyl)–N functionalisation catalysis.

Author contributions

VGP – conceptualization, investigation, writing – original draft, writing – review & editing, visualization. KRM – investigation, writing – review & editing. CRK – conceptualization, writing – original draft, writing – review & editing, visualization, supervision, project administration, funding acquisition.

Data availability

No primary research results, software or code have been included and no new data were generated or analysed as part of this review.

Conflicts of interest

There are no conflicts to declare.

Acknowledgements

Research reported in this publication was supported through start-up funding from the University of Rochester and by the National Institute of General Medical Sciences of the National Institutes of Health under Award Number R35GM150833. The content is solely the responsibility of the authors and does not necessarily represent the official views of the National Institutes of Health. V. G. P. acknowledges the University of Rochester Department of Chemistry for Sherman–Clarke and Weissberger Memorial Fellowships.

References

1 J. I. Mujika, J. M. Matxain, L. A. Eriksson and X. Lopez, *Chem. – Eur. J.*, 2006, **12**, 7215–7224.
2 G. Li, S. Ma and M. Szostak, *Trends Chem.*, 2020, **2**, 914–928.
3 C. Liu and M. Szostak, *Chem. – Eur. J.*, 2017, **23**, 7157–7173.
4 J. E. Dander and N. K. Garg, *ACS Catal.*, 2017, **7**, 1413–1423.
5 T. B. Boit, A. S. Bulger, J. E. Dander and N. K. Garg, *ACS Catal.*, 2020, **10**, 12109–12126.
6 *Amide Bond Activation: Concepts and Reactions*, ed. M. Szostak, Wiley, 2022.
7 Q. Wang, Y. Su, L. Li and H. Huang, *Chem. Soc. Rev.*, 2016, **45**, 1257–1272.
8 K. Ouyang, W. Hao, W.-X. Zhang and Z. Xi, *Chem. Rev.*, 2015, **115**, 12045–12090.
9 E. V. Anslyn and D. A. Dougherty, in *Modern Physical Organic Chemistry*, University Science Books, 2006, ch. 600–607.
10 P. Gao, M. M. Rahman, A. Zamalloa, J. Feliciano and M. Szostak, *J. Org. Chem.*, 2022, **88**(19), 13371–13391.
11 M. Szostak and J. Aube, *Chem. Rev.*, 2013, **113**, 5701–5765.
12 G. Meng, J. Zhang and M. Szostak, *Chem. Rev.*, 2021, **121**, 12746–12783.
13 R. Szostak, S. Shi, G. Meng, R. Lalancette and M. Szostak, *J. Org. Chem.*, 2016, **81**, 8091–8094.
14 L. Ielo, V. Pace, W. Holzer, M. M. Rahman, G. Meng, R. Szostak and M. Szostak, *Chem. – Eur. J.*, 2020, **26**, 16246–16250.
15 R. Szostak, J. Aube and M. Szostak, *Chem. Commun.*, 2015, **51**, 6395–6398.
16 V. Pace, W. Holzer, L. Ielo, S. Shi, G. Meng, M. Hanna, R. Szostak and M. Szostak, *Chem. Commun.*, 2019, **55**, 4423–4426.
17 P. Lei, G. Meng, S. Shi, Y. Ling, J. An, R. Szostak and M. Szostak, *Chem. Sci.*, 2017, **8**, 6525–6530.
18 R. Szostak, G. Meng and M. Szostak, *J. Org. Chem.*, 2017, **82**, 6373–6378.
19 J. M. Buccigross and S. A. Glover, *J. Chem. Soc., Perkin Trans. 2*, 1995, 595–603, DOI: **10.1039/P29950000595**.
20 S. A. Glover, *Tetrahedron*, 1998, **54**, 7229–7271.
21 S. A. Glover, G. Mo and A. Rauk, *Tetrahedron*, 1999, **55**, 3413–3426.
22 S. A. Glover and A. Rauk, *J. Chem. Soc., Perkin Trans. 2*, 2002, 1740–1746, DOI: **10.1039/B204232K**.
23 S. A. Glover, J. M. White, A. A. Rosser and K. M. Digianantonio, *J. Org. Chem.*, 2011, **76**, 9757–9763.
24 S. A. Glover and A. A. Rosser, *Molecules*, 2018, **23**(11), 2834.
25 S. H. Kennedy, B. D. Dherange, K. J. Berger and M. D. Levin, *Nature*, 2021, **593**, 223–227.
26 C. Zippel, J. Seibert and S. Bräse, *Angew. Chem., Int. Ed.*, 2021, **60**, 19522–19524.
27 K. J. Berger, J. L. Driscoll, M. Yuan, B. D. Dherange, O. Gutierrez and M. D. Levin, *J. Am. Chem. Soc.*, 2021, **143**, 17366–17373.

28 B. D. Dherange, M. Yuan, C. B. Kelly, C. A. Reiher, C. Grosanu, K. J. Berger, O. Gutierrez and M. D. Levin, *J. Am. Chem. Soc.*, 2023, **145**, 17–24.
29 C. Lv, R. Zhao, X. Wang, D. Liu, T. Muschin, Z. Sun, C. Bai, A. Bao and Y. S. Bao, *J. Org. Chem.*, 2023, **88**, 2140–2157.
30 A. M. Smith and R. Whyman, *Chem. Rev.*, 2014, **114**, 5477–5510.
31 J. Pritchard, G. A. Filonenko, R. van Putten, E. J. M. Hensen and E. A. Pidko, *Chem. Soc. Rev.*, 2015, **44**, 3808–3833.
32 H. Zhao, A. Ariafard and Z. Lin, *Organometallics*, 2006, **25**, 812–819.
33 V. T. Tran, J. A. Gurak, K. S. Yang and K. M. Engle, *Nat. Chem.*, 2018, **10**, 1126–1133.
34 M. Karimzadeh-Younjali and O. F. Wendt, *Helv. Chim. Acta*, 2021, **104**, e2100114.
35 M. K. Bogdos, O. Stepanović, A. Bismuto, M. G. Luraschi and B. Morandi, *Nat. Synth.*, 2022, **1**, 787–793.
36 E. Balaraman, B. Gnanaprakasam, L. J. W. Shimon and D. Milstein, *J. Am. Chem. Soc.*, 2010, **132**, 16756–16758.
37 C. Gunanathan, Y. Ben-David and D. Milstein, *Science*, 2007, **317**, 790–792.
38 D. Milstein, *Top. Catal.*, 2010, **53**, 915–923.
39 D. Cantillo, *Eur. J. Inorg. Chem.*, 2011, **2011**, 3008–3013.
40 H. Li, X. Wang, F. Huang, G. Lu, J. Jiang and Z.-X. Wang, *Organometallics*, 2011, **30**, 5233–5247.
41 G. Zeng and S. Li, *Inorg. Chem.*, 2011, **50**, 10572–10580.
42 D. Cho, K. C. Ko and J. Y. Lee, *Organometallics*, 2013, **32**, 4571–4576.
43 L. Li, M. Lei, L. Liu, Y. Xie and H. F. Schaefer III, *Inorg. Chem.*, 2018, **57**, 8778–8787.
44 J. M. John and S. H. Bergens, *Angew. Chem., Int. Ed.*, 2011, **50**, 10377–10380.
45 J. M. John, R. Loorthuraja, E. Antoniuk and S. H. Bergens, *Catal. Sci. Technol.*, 2015, **5**, 1181–1186.
46 M. Ito, T. Ootsuka, R. Watari, A. Shiibashi, A. Himizu and T. Ikariya, *J. Am. Chem. Soc.*, 2011, **133**, 4240–4242.
47 T. Miura, I. E. Held, S. Oishi, M. Naruto and S. Saito, *Tetrahedron Lett.*, 2013, **54**, 2674–2678.
48 N. M. Rezayee, C. A. Huff and M. S. Sanford, *J. Am. Chem. Soc.*, 2015, **137**, 1028–1031.
49 J. R. Cabrero-Antonino, E. Alberico, H.-J. Drexler, W. Baumann, K. Junge, H. Junge and M. Beller, *ACS Catal.*, 2016, **6**, 47–54.
50 J. A. Garg, S. Chakraborty, Y. Ben-David and D. Milstein, *Chem. Commun.*, 2016, **52**, 5285–5288.
51 F. Schneck, M. Assmann, M. Balmer, K. Harms and R. Langer, *Organometallics*, 2016, **35**, 1931–1943.
52 L. Shi, X. Tan, J. Long, X. Xiong, S. Yang, P. Xue, H. Lv and X. Zhang, *Chem. – Eur. J.*, 2017, **23**, 546–548.
53 U. Jayarathne, Y. Zhang, N. Hazari and W. H. Bernskoetter, *Organometallics*, 2017, **36**, 409–416.
54 V. Papa, J. R. Cabrero-Antonino, E. Alberico, A. Spanneberg, K. Junge, H. Junge and M. Beller, *Chem. Sci.*, 2017, **8**, 3576–3585.
55 T. Miura, M. Naruto, K. Toda, T. Shimomura and S. Saito, *Sci. Rep.*, 2017, **7**, 1586.
56 T. Leischner, L. Artús Suarez, A. Spannenberg, K. Junge, A. Nova and M. Beller, *Chem. Sci.*, 2019, **10**, 10566–10576.
57 S. Kar, A. Goeppert, J. Kothandaraman and G. K. S. Prakash, *ACS Catal.*, 2017, **7**, 6347–6351.
58 S. Kar, R. Sen, J. Kothandaraman, A. Goeppert, R. Chowdhury, S. B. Munoz, R. Haiges and G. K. S. Prakash, *J. Am. Chem. Soc.*, 2019, **141**, 3160–3170.
59 S. Kar, A. Goeppert and G. K. S. Prakash, *J. Am. Chem. Soc.*, 2019, **141**, 12518–12521.
60 T. He, J. C. Buttner, E. F. Reynolds, J. Pham, J. C. Malek, J. M. Keith and A. R. Chianese, *J. Am. Chem. Soc.*, 2019, **141**, 17404–17413.
61 J. Pham, C. E. Jarczyk, E. F. Reynolds, S. E. Kelly, T. Kim, T. He, J. M. Keith and A. R. Chianese, *Chem. Sci.*, 2021, **12**, 8477–8492.
62 L. N. Dawe, M. Karimzadeh-Younjali, Z. Dai, E. Khaskin and D. G. Gusev, *J. Am. Chem. Soc.*, 2020, **142**, 19510–19522.
63 S. Kar, M. Rauch, A. Kumar, G. Leitus, Y. Ben-David and D. Milstein, *ACS Catal.*, 2020, **10**, 5511–5515.
64 A. Kumar, N. von Wolff, M. Rauch, Y. Q. Zou, G. Shmul, Y. Ben-David, G. Leitus, L. Avram and D. Milstein, *J. Am. Chem. Soc.*, 2020, **142**, 14267–14275.
65 H. Li and M. B. Hall, *ACS Catal.*, 2015, **5**, 1895–1913.
66 W. H. Bernskoetter and N. Hazari, in *Pincer Compounds*, ed. D. Morales-Morales, Elsevier, 2018, ch. 6, pp. 111–131. DOI: 10.1016/B978-0-12-812931-9.00006-2.
67 D. S. Mérel, M. L. T. Do, S. Gaillard, P. Dupau and J.-L. Renaud, *Coord. Chem. Rev.*, 2015, **288**, 50–68.
68 E. M. Lane, K. B. Uttley, N. Hazari and W. Bernskoetter, *Organometallics*, 2017, **36**, 2020–2025.
69 L. Artús Suàrez, Z. Culakova, D. Balcells, W. H. Bernskoetter, O. Eisenstein, K. I. Goldberg, N. Hazari, M. Tilset and A. Nova, *ACS Catal.*, 2018, **8**, 8751–8762.
70 L. Artús Suàrez, U. Jayarathne, D. Balcells, W. H. Bernskoetter, N. Hazari, M. Jaraiz and A. Nova, *Chem. Sci.*, 2020, **11**, 2225–2230.
71 J. B. Curley, N. E. Smith, W. H. Bernskoetter, M. Z. Ertem, N. Hazari, B. Q. Mercado, T. M. Townsend and X. Wang, *ACS Catal.*, 2021, **11**, 10631–10646.
72 A. K. Ravn and N. M. Rezayee, *ACS Catal.*, 2022, **12**, 11927–11933.
73 X. Li and G. Zou, *Chem. Commun.*, 2015, **51**, 5089–5092.
74 G. Meng and M. Szostak, *Org. Lett.*, 2015, **17**, 4364–4367.
75 L. Hie, N. F. Fine Nathel, T. K. Shah, E. L. Baker, X. Hong, Y. F. Yang, P. Liu, K. N. Houk and N. K. Garg, *Nature*, 2015, **524**, 79–83.
76 N. A. Weires, D. D. Caspi and N. K. Garg, *ACS Catal.*, 2017, **7**, 4381–4385.
77 E. L. Baker, M. M. Yamano, Y. Zhou, S. M. Anthony and N. K. Garg, *Nat. Commun.*, 2016, **7**, 11554.
78 N. A. Weires, E. L. Baker and N. K. Garg, *Nat. Chem.*, 2016, **8**, 75–79.

79 L. Hie, E. L. Baker, S. M. Anthony, J. N. Desrosiers, C. Senanayake and N. K. Garg, *Angew. Chem., Int. Ed.*, 2016, **55**, 15129–15132.
80 B. J. Simmons, N. A. Weires, J. E. Dander and N. K. Garg, *ACS Catal.*, 2016, **6**, 3176–3179.
81 J. E. Dander, E. L. Baker and N. K. Garg, *Chem. Sci.*, 2017, **8**, 6433–6438.
82 T. B. Boit, N. A. Weires, J. Kim and N. K. Garg, *ACS Catal.*, 2018, **8**, 1003–1008.
83 J. E. Dander, M. Giroud, S. Racine, E. R. Darzi, O. Alvizo, D. Entwistle and N. K. Garg, *Commun. Chem.*, 2019, **2**, 82.
84 R. R. Knapp, A. S. Bulger and N. K. Garg, *Org. Lett.*, 2020, **22**, 2833–2837.
85 M. M. Mehta, T. B. Boit, J. E. Dander and N. K. Garg, *Org. Lett.*, 2020, **22**, 1–5.
86 T. B. Boit, M. M. Mehta, J. Kim, E. L. Baker and N. K. Garg, *Angew. Chem., Int. Ed.*, 2021, **60**, 2472–2477.
87 A. S. Bulger, D. J. Nasrallah, A. Tena Meza and N. K. Garg, *Chem. Sci.*, 2024, **15**, 2593–2600.
88 J. A. Walker Jr., K. L. Vickerman, J. N. Humke and L. M. Stanley, *J. Am. Chem. Soc.*, 2017, **139**, 10228–10231.
89 A. A. Kadam, T. L. Metz, Y. Qian and L. M. Stanley, *ACS Catal.*, 2019, **9**, 5651–5656.
90 M. T. Koeritz, R. W. Burgett, A. A. Kadam and L. M. Stanley, *Org. Lett.*, 2020, **22**, 5731–5736.
91 A. S. Moore and L. M. Stanley, *Org. Lett.*, 2022, **24**, 8959–8963.
92 J. Hu, M. Wang, X. Pu and Z. Shi, *Nat. Commun.*, 2017, **8**, 14993.
93 J. Hu, Y. Zhao, J. Liu, Y. Zhang and Z. Shi, *Angew. Chem., Int. Ed.*, 2016, **55**, 8718–8722.
94 J. Buchspies, M. M. Rahman and M. Szostak, *Molecules*, 2021, **26**(1), 188.
95 C. Liu and M. Szostak, *Angew. Chem., Int. Ed.*, 2017, **56**, 12718–12722.
96 S. Shi and M. Szostak, *Org. Lett.*, 2016, **18**, 5872–5875.
97 S. Shi and M. Szostak, *Chem. – Eur. J.*, 2016, **22**, 10420–10424.
98 S. Shi, G. Meng and M. Szostak, *Angew. Chem., Int. Ed.*, 2016, **55**, 6959–6963.
99 J. M. Medina, J. Moreno, S. Racine, S. Du and N. K. Garg, *Angew. Chem., Int. Ed.*, 2017, **56**, 6567–6571.
100 H. Yue, L. Guo, S.-C. Lee, X. Liu and M. Rueping, *Angew. Chem., Int. Ed.*, 2017, **56**, 3972–3976.
101 H. Yue, L. Guo, H. H. Liao, Y. Cai, C. Zhu and M. Rueping, *Angew. Chem., Int. Ed.*, 2017, **56**, 4282–4285.
102 W. Srimontree, A. Chatupheeraphat, H.-H. Liao and M. Rueping, *Org. Lett.*, 2017, **19**, 3091–3094.
103 K. R. Rajamanickam and S. Lee, *J. Org. Chem.*, 2024, **89**, 1336–1344.
104 S. Shi, G. Meng and M. Szostak, *Angew. Chem., Int. Ed.*, 2016, **55**, 6959–6963.
105 G. Meng and M. Szostak, *Angew. Chem., Int. Ed.*, 2015, **54**, 14518–14522.
106 P. Lei, G. Meng and M. Szostak, *ACS Catal.*, 2017, **7**, 1960–1965.
107 P. Lei, G. Meng, Y. Ling, J. An, S. P. Nolan and M. Szostak, *Org. Lett.*, 2017, **19**, 6510–6513.
108 S. Shi and M. Szostak, *Org. Lett.*, 2017, **19**, 3095–3098.
109 C. Liu and M. Szostak, *Org. Biomol. Chem.*, 2018, **16**, 7998–8010.
110 C. Liu, R. Lalancette, R. Szostak and M. Szostak, *Org. Lett.*, 2019, **21**, 7976–7981.
111 T. Zhou, C.-L. Ji, X. Hong and M. Szostak, *Chem. Sci.*, 2019, **10**, 9865–9871.
112 S. Shi and M. Szostak, *ACS Omega*, 2019, **4**, 4901–4907.
113 F. Bie, X. Liu, H. Cao, Y. Shi, T. Zhou, M. Szostak and C. Liu, *Org. Lett.*, 2021, **23**, 8098–8103.
114 A. A. Kadam, T. L. Metz, C. M. David, M. T. Koeritz and L. M. Stanley, *J. Org. Chem.*, 2021, **86**, 6863–6868.
115 G. Meng and M. Szostak, *Org. Lett.*, 2016, **18**, 796–799.
116 G. Meng and M. Szostak, *ACS Catal.*, 2017, **7**, 7251–7256.
117 F. Bie, X. Liu, Y. Shi, H. Cao, Y. Han, M. Szostak and C. Liu, *J. Org. Chem.*, 2020, **85**, 15676–15685.
118 Y. Bourne-Branchu, C. Gosmini and G. Danoun, *Chem. – Eur. J.*, 2017, **23**, 10043–10047.
119 W. Li, S. Zhang, X. Feng, X. Yu, Y. Yamamoto and M. Bao, *Org. Lett.*, 2021, **23**, 2521–2526.
120 C. Liu and M. Szostak, *SynOpen*, 2023, **07**, 88–101.
121 A. Dey, S. Sasmal, K. Seth, G. K. Lahiri and D. Maiti, *ACS Catal.*, 2017, **7**, 433–437.
122 K. R. Malyk, V. G. Pillai, W. W. Brennessel, R. Leon Baxin, E. S. Silk, D. T. Nakamura and C. R. Kennedy, *JACS Au*, 2023, **3**, 2451–2457.
123 H. Y. Zhong, D. T. Egger, V. C. M. Gasser, P. Finkelstein, L. Keim, M. Z. Seidel, N. Trapp and B. Morandi, *Nat. Commun.*, 2023, **14**, 5273.
124 J. Derosa, V. T. Tran, V. A. van der Puyl and K. M. Engle, *Aldrichimica Acta*, 2018, **51**, 21–32.
125 H. Wang, S. Q. Zhang and X. Hong, *Chem. Commun.*, 2019, **55**, 11330–11341.
126 L. L. Liu, P. Chen, Y. Sun, Y. Wu, S. Chen, J. Zhu and Y. Zhao, *J. Org. Chem.*, 2016, **81**, 11686–11696.
127 Z. Y. Xu, H. Z. Yu and Y. Fu, *Chem. – Asian J.*, 2017, **12**, 1765–1772.
128 C. L. Ji and X. Hong, *J. Am. Chem. Soc.*, 2017, **139**, 15522–15529.
129 T. Morioka, A. Nishizawa, T. Furukawa, M. Tobisu and N. Chatani, *J. Am. Chem. Soc.*, 2017, **139**, 1416–1419.
130 C. Q. Chu and L. Dang, *J. Org. Chem.*, 2018, **83**, 5009–5018.
131 P.-P. Xie, Z.-X. Qin, S.-Q. Zhang and X. Hong, *ChemCatChem*, 2021, **13**, 3536–3542.
132 A. M. Borys and E. Hevia, *Angew. Chem., Int. Ed.*, 2021, **60**, 24659–24667.
133 J. Terao and N. Kambe, *Acc. Chem. Res.*, 2008, **41**, 1545–1554.
134 A. M. Borys, L. Vedani and E. Hevia, *Dalton Trans.*, 2024, **53**, 8382–8390.
135 H. Y. Tu, S. Zhu, F. L. Qing and L. Chu, *Synthesis*, 2020, 1346–1356.
136 J.-B. Peng, *Adv. Synth. Catal.*, 2020, **362**, 3059–3080.

137 R. Doi, K. Shimizu, Y. Ikemoto, M. Uchiyama, M. Koshiba, A. Furukawa, K. Maenaka, S. Watanabe and Y. Sato, *ChemCatChem*, 2021, **13**, 2086–2092.
138 E. P. Jackson, H. A. Malik, G. J. Sormunen, R. D. Baxter, P. Liu, H. Wang, A.-R. Shareef and J. Montgomery, *Acc. Chem. Res.*, 2015, **48**, 1736–1745.
139 A. D. Jenkins, M. T. Robo, P. M. Zimmerman and J. Montgomery, *J. Org. Chem.*, 2020, **85**, 2956–2965.
140 S. Ohno, J. Qiu, R. Miyazaki, H. Aoyama, K. Murai, J.-y. Hasegawa and M. Arisawa, *Org. Lett.*, 2019, **21**, 8400–8403.
141 S. D. Tambe, N. Iqbal and E. J. Cho, *Org. Lett.*, 2020, **22**, 8550–8554.
142 S. Ogoshi, *Bull. Chem. Soc. Jpn.*, 2017, **90**, 1401–1406.
143 J. Amani, R. Alam, S. Badir and G. A. Molander, *Org. Lett.*, 2017, **19**, 2426–2429.
144 S. Ni, W. Zhang, H. Mei, J. Han and Y. Pan, *Org. Lett.*, 2017, **19**, 2536–2539.
145 G. S. Lee, J. Won, S. Choi, M. H. Baik and S. H. Hong, *Angew. Chem., Int. Ed.*, 2020, **59**, 16933–16942.
146 T. Kerackian, A. Reina, T. Krachko, H. Boddaert, D. Bouyssi, N. Monteiro and A. Amgoune, *Synlett*, 2021, 1531–1536.
147 T. Kerackian, D. Bouyssi, G. Pilet, M. Médebielle, N. Monteiro, J. C. Vantourout and A. Amgoune, *ACS Catal.*, 2022, **12**, 12315–12325.